

# PIEZO2 is required for mechanotransduction in human stem cell–derived touch receptors

Katrin Schrenk-Siemens<sup>1</sup>, Hagen Wende<sup>1</sup>, Vincenzo Prato<sup>1</sup>, Kun Song<sup>1</sup>, Charlotte Rostock<sup>1</sup>, Alexander Loewer<sup>2</sup>, Jochen Utikal<sup>3</sup>, Gary R Lewin<sup>2</sup>, Stefan G Lechner<sup>1</sup> & Jan Siemens<sup>1</sup>

Human sensory neurons are inaccessible for functional examination, and thus little is known about the mechanisms mediating touch sensation in humans. Here we demonstrate that the mechanosensitivity of human embryonic stem (hES) cell–derived touch receptors depends on PIEZO2. To recapitulate sensory neuron development *in vitro*, we established a multistep differentiation protocol and generated sensory neurons via the intermediate production of neural crest cells derived from hES cells or human induced pluripotent stem (hiPS) cells. The generated neurons express a distinct set of touch receptor–specific genes and convert mechanical stimuli into electrical signals, their most salient characteristic *in vivo*. Strikingly, mechanosensitivity is lost after CRISPR/Cas9-mediated *PIEZO2* gene deletion. Our work establishes a model system that resembles human touch receptors, which may facilitate mechanistic analysis of other sensory subtypes and provide insight into developmental programs underlying sensory neuron diversity.

Mechanotransduction, the conversion of mechanical force into electrochemical signals, is the basis for several sensory phenomena, including hearing, balance and touch sensation. Touch receptors are highly specialized sensory neurons that innervate the skin and confer the capacity to discriminate shape and fine texture of objects<sup>1</sup>. *In vivo*, touch receptors, also referred to as low-threshold mechanoreceptors (LTMRs), are intermingled with sensory neurons finely tuned to detect a variety of other thermal and chemical stimuli<sup>2</sup>.

Unlike LTMRs, nociceptors are transducers of high-threshold noxious and painful stimuli and thus constitute a separate category of sensory neurons. These functional differences correlate with the expression of different molecular markers<sup>3</sup>.

The heterogeneity of sensory ganglia and very low abundance of modality-specific sensory neuron subtypes *in vivo* have hampered efforts to isolate and characterize them. Both human nociceptors and LTMRs are inaccessible for functional characterization.

Recent studies describe the generation of nociceptors from hES cells by use of small-molecule inhibitors<sup>4,5</sup>, opening up new possibilities for studying nociceptor function and deriving new cellular disease models relevant for pain therapy. However, no *in vitro* model of human LTMRs has been described, and neuronal mechanisms that mediate rapid transduction of small mechanical stimuli have remained largely elusive.

Two molecules implicated in sensing mechanical force in different cellular contexts are the large transmembrane proteins Piezo1 and Piezo2 (refs. 6–9). Piezo2 is expressed in both nociceptors and LTMRs and is also found in epidermal Merkel cells that are part of terminal touch-receptive specializations<sup>6,8–10</sup>. Indeed, Merkel

cells modulate and tune touch responses of LTMRs in a Piezo2-dependent manner, as shown by specific and restricted Merkel cell knockout and knockdown studies<sup>8–10</sup>. These studies clearly show that Piezo2 conveys mechanical sensitivity to epidermal Merkel cells, but touch responses are not abolished in these mouse models, and it is currently not known whether Piezo2 is a transducer of mechanical stimuli in LTMRs, nociceptors or both.

To examine human touch receptor function, we recapitulated sensory neuron development *in vitro* and established a multistep differentiation protocol to generate LTMRs via the intermediate production of hES cell–derived neural crest (NC) cells, the sensory neuron progenitors<sup>3,11</sup>. The resulting neurons express a highly distinct set of LTMR-specific genes. They also convert mechanical stimuli into electrical signals, their most salient characteristic *in vivo*. The differentiation procedure is not only effective in hES cells but also facilitates the conversion of hiPS cells into LTMRs. Additionally, we find that viral delivery of NGN2, a key transcription factor in sensory neuron development, promotes differentiation and directs a larger fraction of progenitor cells to adopt LTMR fate. Finally, we demonstrate that Piezo2 expression is required for mechanotransduction of hES cell–derived LTMRs.

## RESULTS

### hES cell–derived NC cells generate sensory neurons *in vitro*

*In vivo*, peripheral sensory neurons derive from multipotent NC cells. During development, NC cells delaminate from the neural tube and generate functionally distinct subpopulations of dorsal root ganglion (DRG) neurons in consecutive waves<sup>11,12</sup>. Inducing hES cells to form neuroectodermal spheres mimics key aspects of neural tube formation

<sup>1</sup>Department of Pharmacology, University of Heidelberg, Heidelberg, Germany. <sup>2</sup>Max Delbrück Center for Molecular Medicine, Berlin, Germany. <sup>3</sup>Skin Cancer Unit, German Cancer Research Center (DKFZ), Heidelberg and University Medical Center Mannheim, Mannheim, Germany. Correspondence should be addressed to J.S. (jan.siemens@pharma.uni-heidelberg.de).

Received 6 October; accepted 13 November; published online 3 December 2014; doi:10.1038/nn.3894

**Figure 1** Generation of hES cell–derived sensory neurons. (a) Illustration of the differentiation procedure (top) and sequential image series (bottom) showing one hES cell–derived neuroectodermal sphere and delaminating, migrating NC cells at different time points. (b) Immunocytochemistry showing ISL1 and NF200 expression in NC-descendant cells 2 d *in vitro*. (c,d) Immunocytochemistry and differential interference contrast (d, right) images of derived neurons stained for NF200 at 21 d *in vitro*. Arrowhead and arrow (c) indicate soma and neurite branch point, respectively. Scale bars, 50  $\mu$ m (a–d).

and has been used extensively for the *in vitro* generation of central nervous system neurons<sup>13</sup>. Because NC cells also originate from the neuroectoderm, we asked whether it is possible to obtain NC cells from hES cell–derived neuroectodermal spheres for the subsequent differentiation into sensory neurons.

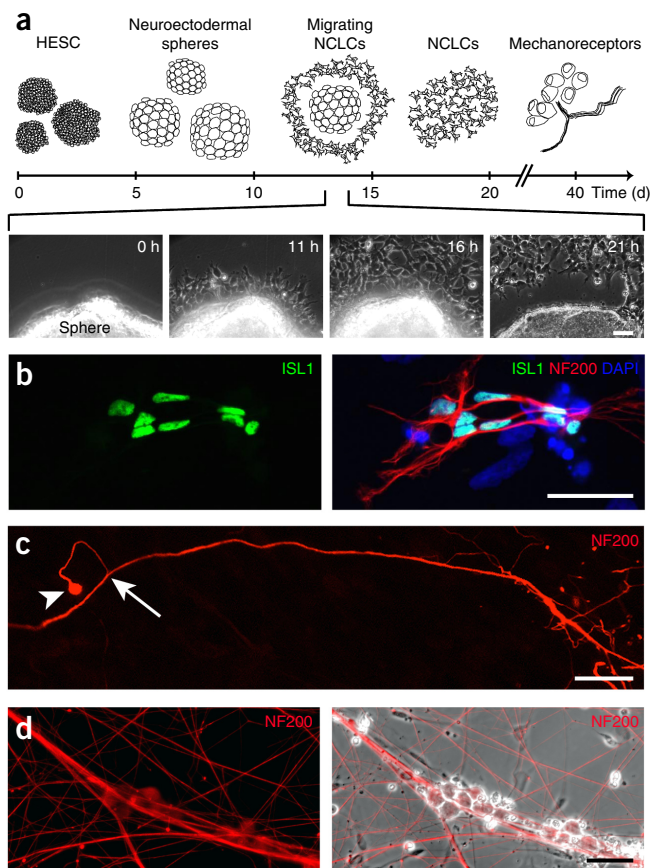
We were intrigued to find that once neuroectodermal spheres formed, a discrete cell population migrated out and became spatially separated from the sphere (Fig. 1a and Supplementary Video 1).

The stellate morphology, migratory phenotype, gene expression profile and differentiation potential, assessed in transplantation experiments, strongly suggested that the derived cells resemble native NC cells<sup>14</sup> (Supplementary Fig. 1a,c).

*In vivo*, migratory NC cells give rise to several different cell and tissue types and do not produce sensory neurons exclusively. We therefore examined whether the derived NC population has the potential to acquire a sensory neuron fate. Indeed, we found that transcripts of *NEUROG1* (also known as *NGN1*), *NEUROG2* (*NGN2*) and *BRN3A* (*POU4F1*), which encode transcription factors that prime NC cells to become sensory neurons<sup>3</sup>, were expressed in the derived NC population (Supplementary Fig. 1b,c). Next to these transcription factors, soluble neurotrophic factors are crucial for the generation and maintenance of discrete sensory neuron lineages. Thus NGF promotes survival and differentiation of nociceptors, whereas the neurotrophic factors GDNF, NT3 and BDNF contribute to the generation and maintenance of LTMRs, finely tuned for discriminative touch<sup>15–18</sup>.

We therefore asked whether a neurotrophin cocktail, consisting of NGF, GDNF, NT3 and BDNF, would promote differentiation of hES cell–derived NC cells into sensory neurons. For the isolation of the derived NCs, we used their migratory phenotype: once a wave of migratory cells had separated from the neuroectodermal source (Fig. 1a), the sphere was dislodged and carefully removed before neurotrophin incubation of the NC cells.

Subsequent to cell cycle exit, the homeobox transcription factor *Isl1* has been found to be among the first sensory neuron specific genes



expressed<sup>19</sup>. As early as 2 d in culture, ISL1 protein was detectable in clusters of NC-descendant cells (Fig. 1b), suggesting that sensory neuron differentiation had commenced. Further incubation for 7–10 d induced a neuron-like morphology in a subset of cells. Strikingly, the derived neuronal cells had very long processes, which arborized extensively. Many of the neuronal cells featured a pseudo-unipolar architecture—a single protruding neurite that splits into two separate branches (Fig. 1c)—characteristic for peripheral sensory neurons *in vivo*. Moreover, most if not all neuronal cells were specifically labeled with antibodies for NF200 (Fig. 1c,d), a neurofilament found in LTMRs and some nociceptors.

### Molecular characterization of hES cell–derived sensory neurons

The segregation of cutaneous sensory neurons into LTMRs and nociceptors coincides with the differential expression of receptors for the aforementioned neurotrophins. The first wave of migratory NC cells generate LTMRs that express the BDNF receptor TrkB, the NT3/4 receptor TrkC and the GDNF receptor Ret. In contrast, cells of the second wave produce mainly TrkA-positive nociceptors that depend on NGF for their survival<sup>11,20</sup>. Intriguingly, in our cultures we did not detect TRKA transcripts or protein, but we observed prominent expression of TRKB as well as low levels of TRKC (Fig. 2), a profile indicative of LTMRs.

**Figure 2** Expression of TRK receptors in hES cell–derived sensory neurons. (a–c) Analysis of TRK expression in hES cell–derived sensory neurons by immunocytochemistry at 21 d *in vitro*. Cells infected with a human TRKA-expressing lentivirus served as positive control for TRKA labeling (c). WT, wild type. (d) qRT-PCR analysis of individual neuronal clusters obtained from cultures at 21 d *in vitro* ( $n = 3$  neuronal clusters; mean  $\pm$  s.e.m.). Scale bars, 50  $\mu$ m (a,c).

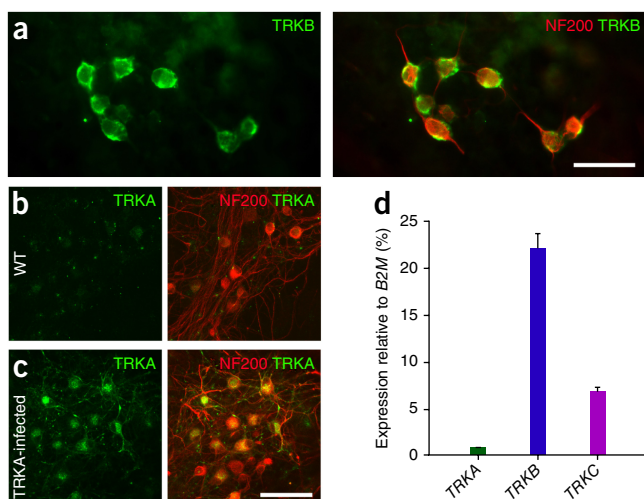
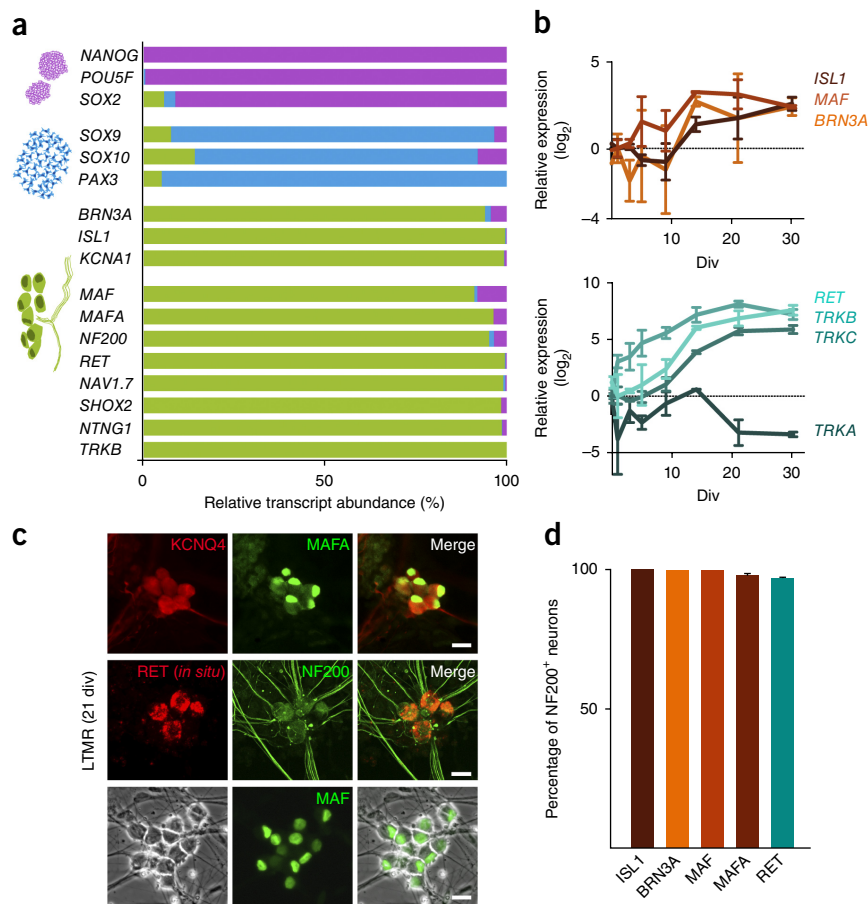


**Figure 3** Molecular characterization of hES cell-derived neurons. **(a)** Global transcriptional profiling by deep sequencing. The relative abundance of transcripts from selected genes is shown for hES cells (purple), NC cells (blue) and human sensory neurons (green). Three biological replicates per cell type were analyzed. **(b)** Time course of marker gene expression in developing hES cell-derived sensory neuron cultures was analyzed by qRT-PCR 0–30 d *in vitro*. (1 d, 5 d, 9 d and 20 d:  $n = 3$ ; 3 d, 14 d and 30 d:  $n = 2$ ). Error bars, mean  $\pm$  s.d. **(c)** Immunocytochemical staining and *in situ* hybridization of differentiated hES cell-derived neurons for markers of mechanoreceptors. Scale bars, 20  $\mu$ m. **(d)** Percentage of coexpression (with NF200) of ‘pansensory’ markers BRN3A and ISL1 and LTMR-specific markers MAFA, MAF and RET in hES cell-derived LTMRs after 21 d *in vitro*. Each marker was quantified by counting double-positive neurons from at least three differentiations. Error bars, mean  $\pm$  s.e.m. Div, days *in vitro*.



Both in rodents and in humans, several functionally distinct subtypes of LTMRs innervate discrete morphological structures in the skin and detect different modalities of touch such as vibration, pressure or skin movement<sup>1</sup>. Transcriptome sequencing (GEO GSE61674) of isolated hES cell-derived neurons as well as immunocytochemistry revealed the expression of MAF, MAFA and the RET receptor (Fig. 3 and Supplementary Fig. 2), a profile highly specific for ‘rapidly adapting’ mechanoreceptors (RA-LTMRs)<sup>16,18,21</sup>.

The deduced RA-LTMR phenotype is also in agreement with the expression of KCNQ4 (Fig. 3c and Supplementary Fig. 2), a voltage-gated channel mutated in patients with impaired RA-LTMR function<sup>22</sup>. Both in humans and mice, KCNQ4 is confined to RA-LTMRs innervating Meissner corpuscles and hair follicle in the skin that confer the capacity to perceive skin movements<sup>1</sup>.

Expression analysis of selected genes at different time points demonstrated that the neurons had adopted a profile highly similar to native RA-LTMRs *in vivo* (Fig. 3b). Three to four weeks after NC cell isolation and culturing, the individual LTMER markers MAF, RET and TRKB had reached stable expression levels, suggesting that the neuronal cells had acquired their terminal phenotype. Moreover, most if not all identified neurons had acquired an identical phenotype and were found to be touch receptors as assessed by marker gene expression (Fig. 3d).

Interestingly, we found that the RET receptor agonist GDNF was sufficient for the generation of hES cell-derived touch receptors, while other neurotrophins were dispensable (complete NT cocktail:  $2.7 \pm 0.4\%$  generated touch receptors; GDNF alone:  $2.8 \pm 1.2\%$ ; No NTs:  $0.01\% \pm 0.01\%$  mean  $\pm$  s.e.m.). This is in agreement with the role of the Ret receptor in the differentiation and maintenance of MafA-positive mouse touch receptors<sup>16,18</sup>.

Although the derived neuronal population appeared to have acquired a homogenous identity, we found a large fraction of slowly dividing, non-neuronal cells in the differentiation cultures. We therefore ascertained whether inhibiting cell proliferation at a time point when post-mitotic sensory neuron precursors had been generated would enrich for touch receptive neurons. Up to 10-fold enrichment of touch receptors over non-neuronal cells was achieved when a

mix of the mitotic blockers FdU (fluorodeoxyuridine) and uridine (10  $\mu$ M each) was included between days 3 and 4 of the differentiation procedure to inhibit proliferating cells. Attempts to further increase yields by interrupting cell proliferation for longer times resulted in premature detachment and death of the neurons, likely reflecting required support of the sensory neurons by non-neuronal cells.

#### Forced expression of NGN2 facilitates generation of LTMRs

Additionally, we explored whether introducing an instructive factor crucial for early sensory neuron development would direct a larger fraction of NC cells to adopt a sensory neuron fate.

Among the essential factors for the early specification of sensory neurons are the aforementioned neurogenins, NGN1 and NGN2. Upon Ngn1 deletion, mice do not generate most types of nociceptors, whereas Ngn2 expression has been associated mostly with the generation of mechanoreceptors<sup>12,16</sup>.

We therefore reasoned that boosting NGN2 expression in NC cells, the sensory neuron progenitors, may increase LTMER yield. To recapitulate the transient expression of NGN2 observed during sensory neuron development *in vivo*<sup>3</sup>, we used a tetracycline-inducible system to limit expression of virally delivered NGN2 to 24 h (ref. 23) (Supplementary Fig. 3).

Two days after induction of NGN2 expression in hES cell-derived NC cells, the number of ISL1-positive sensory neuron precursors was significantly larger than in control uninfected NC cells ( $71.8 \pm 6\%$  in NGN2-infected cells versus  $4.2 \pm 0.9\%$  in uninfected controls mean  $\pm$  s.e.m.,  $P = 0.0002$ ,  $t$ -test (Online Methods)) (Supplementary Fig. 4). Moreover, 21 d after infection of NC cells, the fraction of derived sensory neurons expressing NF200 and ISL1 was significantly higher

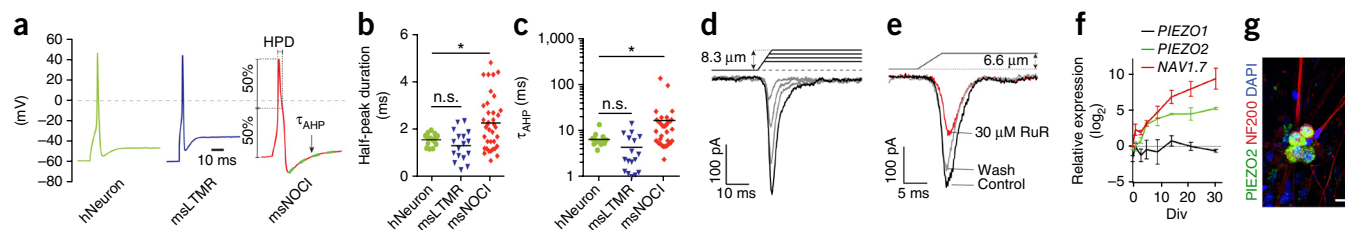


**Figure 4** Functional characterization of hES cell-derived LTMRs. **(a)** Representative examples of action potentials (APs) recorded from hES cell-derived neurons (hNeuron, green trace) and from cultured mouse DRG neurons (mechanoreceptors (msLTMR), blue trace; nociceptors (msNOCI), red trace). HPD, half-peak duration; green dashed line displays the recovery from after-hyperpolarization ( $\tau_{AHP}$ ) fitted with a single exponential decay function. **(b)** AP width quantified as HPD as indicated in **a**. Mean HPDs from hNeurons ( $n = 15$ ), msLTMR ( $n = 17$ ) and msNOCI ( $n = 37$ ) were compared by Mann-Whitney test.  $*P = 0.02$ ; n.s., not significant ( $P = 0.165$ ); mean  $\pm$  s.e.m. **(c)** Recovery from after-hyperpolarization in the same cells was fitted with a single exponential decay function (green dashed line in **a**), and comparison of the deduced time constants ( $\tau_{AHP}$ ) was statistically evaluated by Mann-Whitney test ( $*P = 0.032$ ; n.s.,  $P = 0.054$ ; mean  $\pm$  s.e.m.). **(d)** Representative examples of mechanotransduction currents elicited by mechanical stimuli of increasing magnitude as indicated by the scale above the current traces. **(e)** Application of ruthenium red (RuR,  $30 \mu\text{M}$ ) reversibly attenuated mechanically activated currents by  $40.7 \pm 7.1\%$  (mean  $\pm$  s.e.m.  $n = 5$ ). **(f)** Time course of *PIEZO1*, *PIEZO2* and *NAV1.7* expression during hES cell-derived sensory neuron differentiation analyzed by qRT-PCR 0–30 d *in vitro* (1 d, 5 d, 9 d and 20 d:  $n = 3$ ; 3 d, 14 d and 30 d:  $n = 2$ ). Error bars, mean  $\pm$  s.d. **(g)** *In situ* hybridization and immunocytochemistry of human LTMRs (21 d *in vitro*) labeled for *PIEZO2* (green) and NF200 (red), respectively. Scale bar,  $20 \mu\text{m}$ . 21 div; Div, days *in vitro*.

than in noninfected controls ( $18.7 \pm 2.7\%$  versus  $2.7 \pm 0.4\%$  mean  $\pm$  s.e.m.;  $P = 0.0004$ , *t*-test (Online Methods)). Concurrently, the absolute number of MAFA-positive neurons was substantially higher in the NGN2-infected cells (Supplementary Fig. 4).

These data suggest that the differentiation protocol is versatile and adaptable and the generation of sensory neurons can be directed by the introduction of developmental factors such as NGN2.

#### LTMRs can be generated from hiPS cells

We next asked whether the differentiation protocol is more universally applicable and would enable iPS cells to adopt a sensory neuron fate. We generated an iPS cell line from human skin fibroblasts according to standard protocols<sup>24,25</sup>, and verified its pluripotency through a teratoma formation assay (Supplementary Fig. 5a–c).

Indeed, neuroectodermal spheres generated from hiPS cells give rise to a migratory NC-like cell population that exits the sphere upon contact with the solid support (data not shown). Similar to hES cell-derived NC cells, neurotrophin treatment results in the emergence of

ISL1-positive cells, many of which subsequently acquire a NF200- and MAFA-positive phenotype (Supplementary Fig. 5d–i). Thus, similar to hES cells, hiPS cells can undergo differentiation into mechanoreceptors when subjected to the two-step differentiation protocol.

#### Functional characterization of derived LTMRs

Next, using electrophysiology and  $\text{Ca}^{2+}$  imaging, we tested whether the derived neurons also show functional properties of LTMRs. Cultured rodent nociceptors and touch receptors can be readily distinguished by means of their action potential properties and the absence (LTMRs) and presence (nociceptors) of characteristic responses to pungent chemicals such as capsaicin, mustard oil and menthol.

Upon injection of a depolarizing current, hES cell-derived neurons fired action potentials that were indistinguishable from those recorded from rodent LTMRs but were significantly different from mouse nociceptors<sup>20,26</sup> (Fig. 4a–c). Moreover, voltage-gated sodium currents in hES cell-derived neurons were completely blocked by nanomolar concentrations of tetrodotoxin (TTX) (Supplementary

Fig. 6a), consistent with the presence of  $\text{Na}_v1.7$  (Fig. 3a), a TTX-sensitive sodium channel expressed in LTMRs<sup>27</sup>, whereas the TTX-insensitive nociceptor-specific sodium channels  $\text{Na}_v1.8$  and  $\text{Na}_v1.9$  (refs. 28,29) were absent in the derived neurons (data not shown).

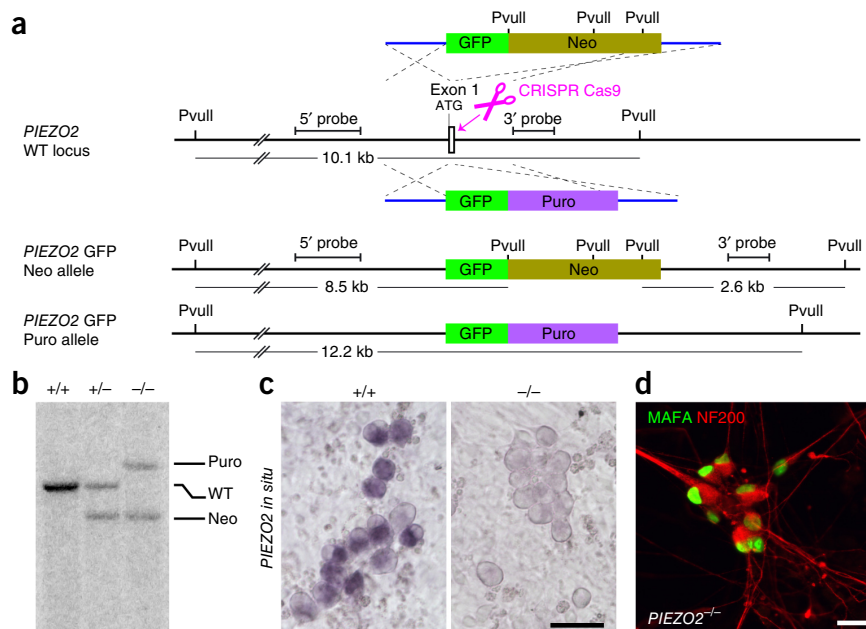


**Figure 5** Generation and characterization of *PIEZO2*-knockout LTMRs. **(a)** Schematic of *PIEZO2* gene deletion using CRISPR/Cas9 and TALEN technology. Neo, neomycin; puro, puromycin. **(b)** Southern blot analysis of hES cell DNA carrying *PIEZO2*<sup>+/+</sup> (WT), *PIEZO2*<sup>+/-</sup> (Neo) and *PIEZO2*<sup>-/-</sup> (Neo and Puro) alleles. (Uncropped blot is presented in Supplementary Fig. 8.) **(c)** *In situ* hybridization for *PIEZO2* in LTMRs derived from *PIEZO2*<sup>+/+</sup> (left) and *PIEZO2*<sup>-/-</sup> (right) hES cells showing absence of transcript in *PIEZO2*<sup>-/-</sup> LTMRs. **(d)** MAFA and NF200 costaining in *PIEZO2*<sup>-/-</sup> hES cell-derived LTMRs after 21 d *in vitro* shows a similar pattern to that of wild-type LTMRs (Fig. 3c); scale bars,  $50 \mu\text{m}$  (c),  $20 \mu\text{m}$  (d).

**Figure 6** Functional analysis of *PIEZO2*-knockout LTMRs. (a) Example traces of action potentials (APs) recorded from *PIEZO2*<sup>+/+</sup> (purple) and *PIEZO2*<sup>-/-</sup> (blue) LTMRs. (b) Characterization of APs from hES cell-derived *PIEZO2*<sup>+/+</sup> and *PIEZO2*<sup>-/-</sup> LTMRs. APs of *PIEZO2*<sup>-/-</sup> neurons (blue) were indistinguishable from APs in *PIEZO2*<sup>+/+</sup> neurons with respect to half-peak duration (left) and recovery from after-hyperpolarization ( $\tau_{\text{AHP}}$ , right). Analysis was as in **Figure 4**. n.s., not significantly different ( $P = 0.31$  (HPD) and  $P = 0.75$  ( $\tau_{\text{AHP}}$ ), Student's *t*-test). (c) Example traces of mechanotransduction currents for the indicated genotypes. Mechanically gated currents were completely absent in *PIEZO2*<sup>-/-</sup> LTMRs. (d) Peak-current amplitudes plotted as a function of mechanical displacement of the membrane. *PIEZO2*<sup>+/+</sup>,  $n = 15$  cells; *PIEZO2*<sup>+/-</sup>,  $n = 15$ ; *PIEZO2*<sup>-/-</sup>,  $n = 46$  (for *PIEZO2*<sup>-/-</sup>, three independent cell clones were analyzed; clone 1,  $n = 18$ ; clone 2,  $n = 16$ ; clone 3,  $n = 12$ ). Error bars, mean  $\pm$  s.e.m.

We did not find any evidence of the expression of other receptors associated with nociceptive function. Both transcriptome sequencing (**Supplementary Table 1**) and calcium imaging (**Supplementary Fig. 6b**) demonstrated that the nociceptor-specific ion channels TRPV1, TRPV4, TRPA1 and TRPM8 (ref. 2) were not present in hES cell-derived neurons.

A fundamental property of mechanoreceptors is mechanotransduction, the ability to convert gentle mechanical stimuli into electrical signals that can be measured electrophysiologically. Rapid membrane indentation by a nanomotor-driven probe (**Supplementary Video 2**) has been shown to elicit a characteristic rapidly adapting (RA) current in isolated mouse LTMRs<sup>20,30</sup>. We found that mechanical stimulation of hES cell-derived neurons elicited robust RA currents, which increased in amplitude as a function of stimulus intensity. Most importantly, the inactivation kinetics of the observed currents ( $\tau = 3.46 \pm 0.79$  ms, mean  $\pm$  s.e.m.) were similar to RA currents observed in mouse mechanoreceptors (**Fig. 4d** and **Supplementary Fig. 7a**).

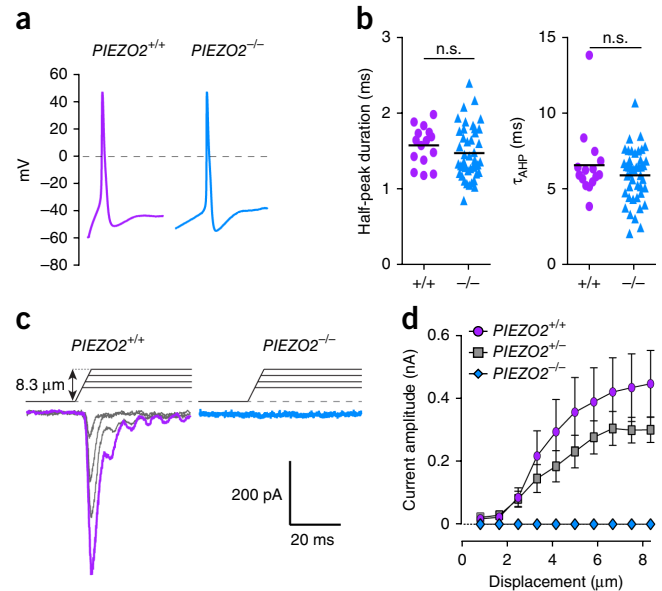
We also examined whether hiPS cell-derived sensory neurons exhibit electrical responses typical for LTMRs. All analyzed hiPS cell-derived sensory neurons exhibited robust mechanically induced currents and electrical properties demonstrated that they had acquired an RA-LTMR phenotype, similar to hES cell-derived neurons (**Supplementary Fig. 7b,c**).

Collectively, the defining molecular characteristics, electrical properties and mechanosensitivity demonstrate that the hES- and hiPS cell-derived neurons share hallmark features of RA-LTMRs.

### Abolition of mechanotransduction currents in *PIEZO2*<sup>-/-</sup> LTMRs

Mechanisms mediating mechanotransduction in LTMRs have not yet been identified. Recently, two mechanically activated ion channels, Piezo1 and Piezo2, were discovered and have been suggested to serve as mechanical force sensors in different cellular contexts including mouse Merkel cells<sup>6-9</sup>.

Interestingly, we found that ruthenium red, an antagonist of Piezo2 and some TRP ion channels<sup>6,8</sup>, attenuated mechanically induced RA currents (**Fig. 4e**). Moreover, transcriptome profiling revealed robust induction of *PIEZO2* (but not *PIEZO1*) during the differentiation of hES cell-derived LTMRs (**Fig. 4f**). After 21 d in culture, *PIEZO2* had reached a stable expression level and *PIEZO1* remained undetectable, as assessed by quantitative reverse transcription PCR (qRT-PCR) (**Fig. 4f**) and deep sequencing (*PIEZO2*:  $77.57 \pm 14$  reads per kilobase per million (RPKM); *PIEZO1*:  $0.89 \pm 0.28$  RPKM; mean  $\pm$  s.e.m.). This finding was corroborated by *in situ* hybridization with an RNA probe specific for human *PIEZO2* transcripts (**Fig. 4g**) and is in agreement with expression of *Piezo2* (and absence of *Piezo1*) in mouse sensory tissue<sup>6</sup>. Also, we found that ruthenium red, an antagonist of *Piezo2* and some TRP ion channels<sup>6,8</sup>,



attenuated mechanically induced RA currents (**Fig. 4e**). On the basis of these results, we considered *PIEZO2* to be a good candidate force transducer in the derived human LTMRs.

To test this hypothesis, we ablated *PIEZO2* from hES cells, using TALEN technology<sup>31</sup> and the CRISPR/Cas9 recombination system<sup>32</sup>. To delete the first coding exon of the *PIEZO2* gene on both chromosomes, we designed two targeting constructs, one harboring a neomycin cassette and the other harboring a puromycin cassette (**Fig. 5a**). Initial transfection with the neomycin-targeting cassette allowed us to obtain heterozygous (*PIEZO2*<sup>+/-</sup>) hES cells, and subsequent transfection of a heterozygous clone with the puromycin-targeting vector enabled us to generate homozygous knockout (*PIEZO2*<sup>-/-</sup>) cells. We verified successful targeting by Southern blot analysis (**Fig. 5b** and **Supplementary Fig. 8**). We chose three independent clones for subsequent experiments to rule out potential unspecific Cas9-mediated DNA damage.

*PIEZO2* transcripts were absent in knockout LTMRs as assessed by *in situ* hybridization (**Fig. 5c**) and qPCR analysis (for *PIEZO2*<sup>+/+</sup>: relative expression of *PIEZO2* transcript is set to  $1 \pm 0.64$ ; *PIEZO2*<sup>-/-</sup>:  $1.53 \times 10^{-4} \pm 6.52 \times 10^{-5}$ ,  $P = 9.8 \times 10^{-4}$ , mean  $\pm$  s.e.m., *t*-test), and transcript levels of *NAV1.7* (*SCN9A*) were comparable to that of wild-type controls (for *PIEZO2*<sup>+/+</sup> relative expression of *NAV1.7* transcript is set to  $1 \pm 0.26$ ; *PIEZO2*<sup>-/-</sup>:  $0.89 \pm 0.35$ ,  $P = 0.81$ ). In addition, the *PIEZO2*<sup>-/-</sup> neurons expressed *MAFA* and *NF200* (**Fig. 5d**). Accordingly, functional examination revealed similar action potential properties in neurons of the different genotypes, suggesting that knockout of *PIEZO2* did not interfere with normal differentiation and electrical excitability of hES cell-derived touch receptors (**Fig. 6a,b**).

Remarkably, RA mechanosensitive currents were entirely absent in all knockout neurons analyzed, which were derived from all three independent hES cell clones (**Fig. 6c,d**). Although not statistically different, heterozygous (*PIEZO2*<sup>+/-</sup>) neurons appeared to have an intermediate phenotype (**Fig. 6d**), probably reflecting a dosage effect and reduced *PIEZO2* expression. Half-maximal activation was reached at a displacement of  $3.43 \pm 0.86$   $\mu\text{m}$  and  $3.58 \pm 0.74$   $\mu\text{m}$  (mean  $\pm$  s.e.m.) for *PIEZO2*<sup>+/+</sup> and *PIEZO2*<sup>+/-</sup>, respectively, as deduced by Boltzmann fitting of the current-displacement curve (**Supplementary Fig. 9**).

In the *PIEZO2*<sup>-/-</sup> neurons, even the largest possible indentation of the plasma membrane did not elicit any current. These findings

demonstrate that PIEZO2 is indispensable for mechanotransduction in human ES cell-derived touch receptors.

## DISCUSSION

The ability to discriminate different types of noxious and innocuous sensations is reflected in a plethora of specialized sensory neurons, posing a challenge to the analysis of their differentiation and function. The stepwise differentiation of hES (or iPS) cells described here is, to our knowledge, the first of its kind to adequately model development and function of a specific type of human touch receptor. Using this model, we provide direct evidence that PIEZO2 is essential for fast mechanotransduction in touch receptors.

It will be interesting to compare these findings with *in vivo* analysis of Piezo2 using appropriate animal models. As Piezo2 is expressed in mouse LTMRs and nociceptors, the receptor may contribute to detecting low- and high-threshold mechanical stimulation, the latter of which mediates the perception of painful stimuli.

The derived RA-LTMRs recapitulate—to the extent that they are known—the molecular profile and functional properties of native touch receptors. Moreover, RA-LTMRs seemed to be the only neuronal cell population in the hES cell-derived cultures and could easily be spotted and harvested. Thus, this model constitutes a valuable tool to dissect the molecular mechanotransduction machinery under physiological conditions as well as in the presence of disease-causing *PIEZO2* mutations<sup>33,34</sup>. In particular, the differentiation protocol described is applicable to hES and hiPS cells, opening up the possibility of studying sensory neuron function in humans. The use of hiPS cells will allow the generation and characterization of sensory neurons from patients who have genetic mutations that affect sensory neuron development and function.

Interestingly, nociceptors appeared not to be present in cultures derived from hES or hiPS cells, despite the presence of NGF in the differentiation cocktail. This correlated with the absence of the high-affinity NGF receptor TRKA.

Notably, *in vivo*, different sensory neuron subtypes are generated from successive waves of delaminating NC cells; LTMRs are generated during the first wave and TrkA-positive nociceptors follow in a subsequent wave<sup>11</sup>. It will be interesting to see whether the neuroectodermal sphere can be induced to generate successive waves of migratory NCs to produce different sensory subtypes, including nociceptors, and whether this correlates with the early emergence of specific developmental genes. Such analysis may help to elucidate a longstanding question about the extent to which sensory neurons are predestined or, alternatively, driven by extrinsic cues to adopt a specific sensory phenotype.

Our experiments with viral infections suggest that induction of NGN2 expression in the derived NC cells facilitates their differentiation into LTMRs. Future studies should show whether viral delivery of other developmental genes, such as *NGN1*, directs sensory-primed NC cells into different sensory subtypes such as nociceptors.

Complementary to existing protocols that derive sensory neurons directly from hES cells by the use of small molecules<sup>4,5</sup>, our work describes the utilization of hES cell-derived NC cells for the *in vitro* generation of sensory neurons. Both approaches, in combination with iPS cell technology as well as viral- and CRISPR/Cas9-mediated genetic manipulation, constitute a versatile toolbox to study sensory neuron diversity and function.

## METHODS

Methods and any associated references are available in the [online version of the paper](#).

**Accession codes.** Gene Expression Omnibus: transcriptome sequencing of isolated hES cell-derived neurons has been deposited under accession code [GSE61674](#).

*Note: Any Supplementary Information and Source Data files are available in the online version of the paper.*

## ACKNOWLEDGMENTS

We thank J. Rossius for help with generating the targeting constructs, C. Birchmeier, T.J. Jentsch and T.C. Südhof for providing antisera and viral expression constructs, V. Benes and J. Blake from the Genomics Core Facility, EMBL Heidelberg, for advice concerning design and analysis of the deep sequencing experiment, and A. Littlewood-Evans for critical reading of the manuscript. This work was supported by the European Research Council (ERC grant agreement 280565), the Alexander von Humboldt Foundation (AvH), the Human Frontiers Science Program (HFSP) (to J.S.) and the German Research Foundation (grant LE3210/2-1 to S.G.L.). Additional support was provided by the German Research Foundation (SFB665 to G.R.L. and SFB873 to J.U.).

## AUTHOR CONTRIBUTIONS

K.S.-S. designed and conducted the differentiation protocol, performed all cell culture work, generated the *PIEZO2* knockout cell line and performed immunocytochemistry and qPCR experiments. H.W. analyzed the deep-sequencing and qPCR data, carried out *in situ* hybridization and helped with the targeting strategy. V.P. conducted the electrophysiological recordings. K.S. prepared the samples for deep-sequencing analysis and performed Ca<sup>2+</sup> imaging. C.R. performed viral infections and Southern blot analysis. A.L. generated **Supplementary Video 1**. J.U. established the iPS cell line. S.G.L. designed and analyzed the electrophysiological recordings. G.R.L., S.G.L., K.S.-S. and H.W. contributed to the editing of the manuscript. J.S. designed experiments and wrote the manuscript.

## COMPETING FINANCIAL INTERESTS

The authors declare no competing financial interests.

Reprints and permissions information is available online at <http://www.nature.com/reprints/index.html>.

1. Abraira, V.E. & Ginty, D.D. The sensory neurons of touch. *Neuron* **79**, 618–639 (2013).
2. Basbaum, A.I., Bautista, D.M., Scherrer, G. & Julius, D. Cellular and molecular mechanisms of pain. *Cell* **139**, 267–284 (2009).
3. Lallemand, F. & Ernfors, P. Molecular interactions underlying the specification of sensory neurons. *Trends Neurosci.* **35**, 373–381 (2012).
4. Chambers, S.M. *et al.* Combined small-molecule inhibition accelerates developmental timing and converts human pluripotent stem cells into nociceptors. *Nat. Biotechnol.* **30**, 715–720 (2012).
5. Young, G.T. *et al.* Characterizing human stem cell-derived sensory neurons at the single-cell level reveals their ion channel expression and utility in pain research. *Mol. Ther.* **22**, 1530–1543 (2014).
6. Coste, B. *et al.* Piezo1 and Piezo2 are essential components of distinct mechanically activated cation channels. *Science* **330**, 55–60 (2010).
7. Coste, B. *et al.* Piezo proteins are pore-forming subunits of mechanically activated channels. *Nature* **483**, 176–181 (2012).
8. Maksimovic, S. *et al.* Epidermal Merkel cells are mechanosensory cells that tune mammalian touch receptors. *Nature* **509**, 617–621 (2014).
9. Woo, S.H. *et al.* Piezo2 is required for Merkel-cell mechanotransduction. *Nature* **509**, 622–626 (2014).
10. Ikeda, R. *et al.* Merkel cells transduce and encode tactile stimuli to drive Abeta-afferent impulses. *Cell* **157**, 664–675 (2014).
11. Marmigère, F. & Ernfors, P. Specification and connectivity of neuronal subtypes in the sensory lineage. *Nat. Rev. Neurosci.* **8**, 114–127 (2007).
12. Ma, Q., Fode, C., Guillemot, F. & Anderson, D.J. Neurogenin1 and neurogenin2 control two distinct waves of neurogenesis in developing dorsal root ganglia. *Genes Dev.* **13**, 1717–1728 (1999).
13. Schwartz, P.H., Brick, D.J., Stover, A.E., Loring, J.F. & Muller, F.J. Differentiation of neural lineage cells from human pluripotent stem cells. *Methods* **45**, 142–158 (2008).
14. Bajpai, R. *et al.* CHD7 cooperates with PBAF to control multipotent neural crest formation. *Nature* **463**, 958–962 (2010).
15. Airaksinen, M.S. *et al.* Specific subtypes of cutaneous mechanoreceptors require neurotrophin-3 following peripheral target innervation. *Neuron* **16**, 287–295 (1996).
16. Bourane, S. *et al.* Low-threshold mechanoreceptor subtypes selectively express MafA and are specified by Ret signaling. *Neuron* **64**, 857–870 (2009).
17. Carroll, P., Lewin, G.R., Koltzenburg, M., Toyka, K.V. & Thoenen, H. A role for BDNF in mechanosensation. *Nat. Neurosci.* **1**, 42–46 (1998).

18. Luo, W., Enomoto, H., Rice, F.L., Milbrandt, J. & Ginty, D.D. Molecular identification of rapidly adapting mechanoreceptors and their developmental dependence on ret signaling. *Neuron* **64**, 841–856 (2009).
19. Sun, Y. *et al.* A central role for *Islet1* in sensory neuron development linking sensory and spinal gene regulatory programs. *Nat. Neurosci.* **11**, 1283–1293 (2008).
20. Lechner, S.G., Frenzel, H., Wang, R. & Lewin, G.R. Developmental waves of mechanosensitivity acquisition in sensory neuron subtypes during embryonic development. *EMBO J.* **28**, 1479–1491 (2009).
21. Wende, H. *et al.* The transcription factor c-Maf controls touch receptor development and function. *Science* **335**, 1373–1376 (2012).
22. Heidenreich, M. *et al.* KCNQ4 K(+) channels tune mechanoreceptors for normal touch sensation in mouse and man. *Nat. Neurosci.* **15**, 138–145 (2012).
23. Zhang, Y. *et al.* Rapid single-step induction of functional neurons from human pluripotent stem cells. *Neuron* **78**, 785–798 (2013).
24. Maherali, N. *et al.* A high-efficiency system for the generation and study of human induced pluripotent stem cells. *Cell Stem Cell* **3**, 340–345 (2008).
25. Somers, A. *et al.* Generation of transgene-free lung disease-specific human induced pluripotent stem cells using a single excisable lentiviral stem cell cassette. *Stem Cells* **28**, 1728–1740 (2010).
26. Rose, R.D., Koerber, H.R., Sedivec, M.J. & Mendell, L.M. Somal action potential duration differs in identified primary afferents. *Neurosci. Lett.* **63**, 259–264 (1986).
27. Ho, C. & O'Leary, M.E. Single-cell analysis of sodium channel expression in dorsal root ganglion neurons. *Mol. Cell. Neurosci.* **46**, 159–166 (2011).
28. Akopian, A.N. *et al.* The tetrodotoxin-resistant sodium channel SNS has a specialized function in pain pathways. *Nat. Neurosci.* **2**, 541–548 (1999).
29. Amaya, F. *et al.* The voltage-gated sodium channel Na<sub>v</sub>1.9 is an effector of peripheral inflammatory pain hypersensitivity. *J. Neurosci.* **26**, 12852–12860 (2006).
30. Poole, K., Herget, R., Lapatsina, L., Ngo, H.D. & Lewin, G.R. Tuning Piezo ion channels to detect molecular-scale movements relevant for fine touch. *Nat. Commun.* **5**, 3520 (2014).
31. Hockemeyer, D. *et al.* Genetic engineering of human pluripotent cells using TALE nucleases. *Nat. Biotechnol.* **29**, 731–734 (2011).
32. Mali, P., Esvelt, K.M. & Church, G.M. Cas9 as a versatile tool for engineering biology. *Nat. Methods* **10**, 957–963 (2013).
33. Coste, B. *et al.* Gain-of-function mutations in the mechanically activated ion channel PIEZO2 cause a subtype of distal arthrogryposis. *Proc. Natl. Acad. Sci. USA* **110**, 4667–4672 (2013).
34. McMillin, M.J. *et al.* Mutations in *piezo2* cause Gordon syndrome, Marden-Walker syndrome, and distal arthrogryposis type 5. *Am. J. Hum. Genet.* **94**, 734–744 (2014).

## ONLINE METHODS

**Stem cell culture and differentiation.** Human embryonic stem cells (HUES-7 line; Harvard University; approved by the German Central Ethics Committee for Stem Cell Research, #1710-79-1-4-51-A01) were cultured on Matrigel-coated (BD Biosciences) dishes in mTeSR1 medium (STEMCELL Technologies) at 37 °C with 5% CO<sub>2</sub>. Cells were split after 3–5 d, depending on colony size, using Accutase (Sigma). Colonies were scraped off and transferred to freshly coated Matrigel dishes. Medium was changed every day.

For neuroectodermal sphere formation, cells were transferred to noncoated dishes in mTeSR1 medium. The medium was changed the next day to sphere medium, containing DMEM/F12, Neurobasal, B27, N2, glutamine (all from Invitrogen) and insulin (Sigma) in the presence of human FGF and human EGF in a concentration of 20 ng per ml (Peprotech). The medium was changed every other day. Spheres spontaneously attached and neural crest (NC) cells migrated out after 6–9 d in culture. For harvesting the NC cells, attached spheres were manually dislodged and carefully removed with a pipette tip under the microscope, and adherent cells were isolated by Accutase treatment. Cells were collected in sphere medium, spun at 1,000 r.p.m. for 4 min and replated on glass coverslips or dishes coated with poly-ornithine (15 µg/ml; Sigma), fibronectin (15 µg/ml; Invitrogen) and laminin (15 µg/ml; Sigma). Cells were plated in a density of 50,000 cells per square centimeter in differentiation medium (sphere medium containing human NGF, NT-3, BDNF and GDNF (Peprotech) in a concentration of 10 ng/ml and retinoic acid (50 nM; Sigma)). The medium was changed every other day. After 10–12 d morphologically distinct mechanoreceptors were visually identifiable by light microscope.

On the basis of available evidence (marker gene profile, electrical properties), derived neurons were fully functional after 3 weeks of differentiation. Therefore, all characterizations were done with cells cultured for a minimum of 21 d *in vitro* (div).

Cell density is a crucial point for the generation of mechanoreceptors, as plating low numbers of NC cells resulted in detachment and death of the neurons and plating too many NC cells resulted in cultures densely populated by other, slowly proliferating, non-neuronal cell types.

**Recording migrating neural crest cells.** For live cell time-lapse microscopy, neuroectodermal spheres were imaged on a Nikon Ti inverted microscope with a 10× plan-apochromat objective and a Hamamatsu Orca R2 camera using differential interference contrast. The microscope was enclosed in an environmental chamber controlling temperature, atmosphere (5% CO<sub>2</sub>) and humidity. Images were acquired every 15 min using Nikon Elements software. Single frames from one time series are shown in **Figure 1**.

**Virus generation.** Lentiviruses were produced in HEK293TN cells (Biocat) by cotransfection with three helper plasmids (pRSV-REV, pMDLg/pRRE and pMD2.G) plus the lentiviral vector DNA (FUW-TetO-Ngn2-P2A-EGFP-T2A-Puro or FUW-rTA, obtained from T. Südhof using calcium phosphate transfection. Lentivirus-containing medium was harvested 48 h and 72 h after transfection, centrifuged (800 × *g* for 20 min) and filtered (0.45 µm pore size).

Virus was subsequently concentrated by mixing the filtered supernatant with 50% PEG-8000 (Sigma) in a ratio of 4:1 and placed at 4 °C overnight. The concentrated viral particles were pelleted by two centrifugation steps (2,500 r.p.m. for 20 min followed by 1,200 r.p.m. for 5 min), resuspended in 200 µl PBS and stored at –80 °C.

**NC cell infection.** For NC cell infection cells were plated on coated glass coverslips in differentiation medium as described above.

24 h after plating, cells were infected with a cocktail consisting of concentrated viral particles (0.6 µl/0.33 cm<sup>2</sup>), HEPES (10 mM) and protamine sulfate (8 µg/ml; Sigma). 24 h later, cells were washed twice with PBS and cultured in fresh differentiation medium. Doxycycline (2 µg/ml, Sigma) was added for 24 h to induce *tetO* gene expression.

**Immunocytochemistry.** Mechanoreceptors differentiated on glass coverslips or on dishes were fixed with 4% PFA for 10 min at room temperature (RT). Cells were washed with PBS and blocked in 10% serum (goat or donkey) for 1 h at RT. Primary and secondary antibodies were applied in buffer containing 3% serum

and 0.1% Triton X-100. Incubation with primary antibody was usually done overnight at 4 °C and with secondary antibody for 2 h at RT. Before mounting, cells were stained with DAPI. Coverslips were mounted in Immu-Mount (Thermo Scientific).

**Antibodies.** Primary antibodies used were rabbit anti-MAFA, rabbit anti-MAF and guinea pig anti-MAF<sup>21</sup> (obtained from C. Birchmeier) (1:20,000, 1:5,000 and 1:5,000), chicken anti-NF200 (Abcam #ab72996, 1:25,000), mouse anti-ISLET-1 (Developmental Studies Hybridoma Bank #39.4D5, 1:100), rabbit anti-TRKB-ATTO-488 (Alomone labs #ANT-019-AG, 1:50), rabbit anti-TRKA (EPITOMICS #2244-1, 1:100), rabbit anti-KCNQ4 (ref. 22) (obtained from T. Jentsch) (1:200), mouse anti-HNK1 (Sigma #C6680, 1:250), rabbit anti-BRN3A (Millipore #AB5945, 1:500), rabbit anti-P75 (Millipore #AB1554, 1:250).

Alexa 488-, 555- and 647-conjugated secondary antibodies were obtained from Molecular Probes. Fluorescence images were taken on a Zeiss Axio Observer A.1 inverted microscope using a Hamamatsu Orca R2 camera or on an A1R or C2+ confocal microscope (Nikon imaging center Heidelberg).

**Data analysis.** Immunocytochemistry for the indicated markers was performed on at least three independent differentiations. For quantification of LTMRs, cells were stained after at least 21 div, and random pictures were quantified from at least three differentiations.

**In situ hybridization.** *In situ* probes were amplified using primers for human *PIEZO2* (hPIEZO2\_Fw: gacCTCGAGCTTCAAACAGATCCCAAAGA and hPIEZO2\_Rv gacGCGGCCGCGAGTCTGTGTCTAAGGTTTCAA) comprising exons 40–51 and human *RET* (hRETUTR\_Fw gacCTCGAG-CACGAGAGCTGATGGCACTAAC and hRETUTR\_Rv gacGCGGCCGCGT-GGCTGCTCAGTACCGAACAC) located in the last exon and 3' UTR. Both probes were cloned into pBluescript SK(+). *In situ* hybridization was performed as previously described<sup>21</sup>.

**Quantitative RT-PCR and transcriptome sequencing.** *Large-scale RNA preparations.* Total RNA was prepared from hES cell-derived NC cells and mechanoreceptors grown on 3.5-cm culture dishes. For the time course of marker expression (**Figs. 3b** and **4f**), time points 1 d, 5 d, 9 d and 21 d were derived from three differentiations, and time points 3 d, 14 d and 30 d were derived from two differentiations. For the analysis of NC cells (**Supplementary Fig. 1a,b**), RNA was derived from one differentiation. RNA was isolated using TRIzol reagent (Invitrogen). cDNA synthesis was performed using the High Capacity RNA-to-cDNA Kit from ABI, Life Technologies.

*Few-cell RNA preparation and amplification for transcriptome sequencing and qRT-PCR.* hES cell-derived NC cells were dissociated and counted. Three samples of 100 cells each were snap frozen in liquid nitrogen (*n* = 3). Three samples of hES-cell-derived sensory neuron clusters (each containing 10–20 LTMRs; *n* = 3), either from *PIEZO2*<sup>+/+</sup> or *PIEZO2*<sup>-/-</sup> hES cells, were picked with a glass pipette and micromanipulator support. After cell isolation, the pipette was crushed in an Eppendorf tube and snap frozen in liquid nitrogen. RNA was isolated using PicoPure (Life Technologies) and RNA quality was analyzed using Bioanalyzer (Agilent). RNA from clusters was amplified using Ovation RNA Amplification System V2 (NuGEN) according to the manufacturer's protocol.

**Quantitative RT-PCR.** cDNA derived from whole cell lysates, NC cells or neuronal clusters was used for qPCR using either inventoried TaqMan assays (ABI) and FastStart Essential DNA Probes Master Mix (Roche) or self-designed primers and Power SYBR Green PCR Master Mix (ABI, Life Technologies). qPCR reactions were performed on a Roche LightCycler 96.

qRT-PCR was performed using the individual samples in technical triplicates (**Supplementary Fig. 1a,b**) or technical duplicates (**Figs. 3b** and **4f**).

Inventoried TaqMan assays for the following genes were used: *SOX9* (Hs01001343\_g1), *SOX10* (Hs00366918\_m1), *PAX3* (Hs00240950\_m1), *P75* (00609977\_m1), *BRN3A* (Hs00366711\_m1), *NEUROGENIN1* (*NGN1*) (Hs01029249\_s1), *NEUROGENIN2* (*NGN2*) (Hs00702774\_s1), *TRKA* (Hs01021011\_m1), *TRKB* (Hs00178811\_m1), *TRKC* (Hs00176797\_m1), *ISL1* (Hs00158126\_m1), *MAF* (Hs04185012\_s1), *RET* (Hs01120030\_m1), *PIEZO1* (Hs00207230\_m1), *PIEZO2* (Hs00401026\_1) and *NAV1.7* (Hs00161567\_m1). As 'housekeeping' genes, *B2M* (Hs00984230\_m1) or *TBP* (Hs00427620\_m1) were used.

The following primers were used for SYBR Green assays: *PIEZO2*\_Exon1\_forward, GGCTCAGAAGTGGTGTGCG; *PIEZO2*\_Exon2\_reverse, GGAGAGCCCATTGTATCGGA; *TBP*\_forward, CCACGCCAGCTTCGGA GAG; *TBP*\_reverse, CAGCAACCGCTTGGGATTATA.

**Data analysis.** For data analysis, relative expression of genes of interest from whole cell culture lysates (Figs. 3 and 4 and **Supplementary Fig. 1**) or low cell amount lysates (Fig. 2 and analysis of *PIEZO2* and *NAV1.7* transcript in *PIEZO2*<sup>+/+</sup> versus *PIEZO2*<sup>-/-</sup> LTMrs) were normalized to the housekeeping genes *B2M* or *TBP*.

Differential expression was analyzed using the comparative Ct ( $\Delta\Delta C_t$ ) method and *t*-tests, if applicable, were performed on  $\Delta C_t$  values.

**Deep-sequencing analysis.** Transcriptome profiling by deep sequencing was performed with cDNA generated from neuronal clusters and dissociated human NC cells (described above). Library construction and deep sequencing was performed at the EMBL core facility (Heidelberg).

Raw reads were aligned using ELAND in the Illumina CASAVA pipeline. BAM files were processed using SAMtools<sup>35</sup>. Read counts were generated using HTSeq<sup>36</sup> and a UCSC Refseq HG19 gene model. For comparison of expression levels between different samples, all read counts were normalized to 1 million reads per sample and the transcript length (reads per kilobase per million reads, RPKM). Differential expression was analyzed using DESeq<sup>37</sup>.

**Data analysis.** For data analysis in **Figure 3a**, the sum of the average reads of a given transcript from hES cells, hNC cells as well as human sensory neurons and LTMrs was calculated. Relative abundance of each transcript within a given cell type was displayed. For **Supplementary Figure 2**, transcript abundance of selected genes is shown as mean RPKM  $\pm$  s.e.m. Access to the entire deep sequencing data set is available in the GEO database under accession code GSE61674.

**Primary cultures of DRG neurons.** All animal work was approved by the Ethics and Animal Welfare Committee of the University of Heidelberg and the State of Baden-Wuerttemberg. C57BL/6 female mice at 6 weeks of age were sacrificed using isoflurane and decapitation. DRGs from all spinal segments were collected in Ca<sup>2+</sup>- and Mg<sup>2+</sup>-free PBS. DRGs were subsequently treated with collagenase IV (1 mg/ml; Sigma-Aldrich) and trypsin (0.05%, Invitrogen) at 37 °C for 30 min and 40 min, respectively. After enzyme treatment, DRGs were washed twice with growth medium (DMEM-F12 (Invitrogen)) supplemented with L-glutamine (2  $\mu$ M; Sigma-Aldrich), glucose (8 mg/ml, Sigma-Aldrich), penicillin (200 U/ml), streptomycin (200  $\mu$ g/ml; Invitrogen) and 5% FHS (Invitrogen), triturated using fire-polished Pasteur pipettes and plated in a droplet of growth medium on a glass coverslip precoated with poly-L-lysine (20  $\mu$ g/cm<sup>2</sup>; Sigma-Aldrich) and laminin (4  $\mu$ g/cm<sup>2</sup>; Invitrogen). To allow neurons to adhere, coverslips were kept for 3–4 h at 37 °C in a humidified incubator before being flooded with fresh growth medium. Cultures were used for patch-clamp experiments the next day.

**Patch clamp recordings.** Whole cell patch clamp recordings were performed at room temperature (20–24 °C). Patch pipettes were pulled (Flaming-Brown puller, Sutter Instruments, Novato, CA, USA) from borosilicate glass capillaries (Hilgenberg, Malsfeld, Germany), filled with a solution consisting of (mM) KCl (110), NaCl (10), MgCl<sub>2</sub> (1), EGTA (1) and HEPES (10), adjusted to pH 7.3 with KOH and had tip resistances of 2–3 M $\Omega$ . The bathing solution contained (mM) NaCl (140), KCl (4), CaCl<sub>2</sub> (2), MgCl<sub>2</sub> (1), glucose (4), HEPES (10), adjusted to pH 7.4 with NaOH. Drugs were applied with a gravity driven multi-barrel perfusion system (ValveLink8.2, AutoMate Scientific Inc.). All recordings were made using an EPC-10 amplifier (HEKA, Lambrecht, Germany) in combination with Patchmaster and Fitmaster software (HEKA). Pipette and membrane capacitance were compensated using the auto function of Patchmaster and series resistance was compensated by 70% to minimize voltage errors.

Mechanically activated currents were recorded as previously described<sup>17</sup>. Briefly, neurons were clamped to –60 mV, stimulated mechanically with a fire-polished glass pipette (tip diameter 2–3  $\mu$ m) that was mounted to a piezo-driven micromanipulator (Nanomotor, MM3A, Kleindiek Nanotechnik, Reutlingen, Germany) and the evoked whole cell currents were recorded with a sampling frequency of 200 kHz. The stimulation probe was positioned at an angle of 45° to the surface of the dish and moved with a velocity of 1.33  $\mu$ m/ms. Currents were fit with single exponential functions and classified as RA-, IA- and SA-type currents

according to their inactivation time constant. For **Supplementary Figure 8** currents were fitted to a Boltzmann function with constraint bottom = 0. Cells were classified as mechanically insensitive when stimuli  $\geq 8.3$   $\mu$ m did not elicit a response. Recordings in which the gigaseal was lost before stimuli  $\geq 8.3$   $\mu$ m were applied were not considered for our analysis. For classification of mouse sensory neurons, action potentials were evoked by repetitive 80 ms current injections increasing from 40 pA to 800 pA in increments of 40 pA.

**Ca<sup>2+</sup> imaging.** Ca<sup>2+</sup> imaging was performed using dispersed 1-d-old DRG cultures (prepared as stated above) and 21-d-old hES cell-derived sensory neurons. Cells were loaded with Fura-2 (Sigma) for 1 h at RT and washed with Ringer solution. Fluorescent images were acquired with Metafluor Software (Molecular Devices) and analyzed with GraphPad Prism Software. Cells were challenged with hypotonic solution (45%), menthol (500  $\mu$ M; Sigma), mustard oil (allyl-isothiocyanate, 200  $\mu$ M; Sigma) and capsaicin (1  $\mu$ M; Sigma). Depolarization by a high-potassium solution was used to visualize all neurons in the culture. For analysis, the average normalized fluorescence ratios ( $F_{340}/F_{380}$ ) for capsaicin-only responsive neurons ( $n = 19$ ), mustard oil + capsaicin responsive neurons ( $n = 8$ ;) and menthol-only responsive neurons ( $n = 3$ ) of mouse DRG as well as hES cell-derived sensory neurons ( $n = 17$ ) were calculated and shown as traces (**Supplementary Fig. 6b**).  $F_{340}/F_{380}$  for hypotonic solution-responsive mouse DRG neurons ( $n = 10$ ) together with hES cell-derived neurons ( $n = 3$ ) are shown in **Supplementary Figure 6b**.

**Generation of *PIEZO2* knockout hES cells.** The *PIEZO2*<sup>-/-</sup> hES cell lines were generated by homologous recombination, using CRISPR/Cas9 and TALEN technology. *PIEZO2* specific target sites for CRISPR/Cas9 were designed using the CRISPR Design Tool. The oligonucleotides (CACCGTGGTGTGCGGGCT CATCTTC-forw; AAACGAAGATGAGCCCGCACACCAC-rev) were cloned into CRISPR:hSpCas9 (px330; Addgene) and used for electroporation. *PIEZO2*-specific target sites using TALEN technology were designed by Cellctis bioresearch, Paris. The sequences of the TALEN pair are as follows: left TAL effector DNA-binding domain: TGGCCTCAGAAGTGGTG, right TAL effector DNA-binding domain: CAGGCTGCTGCTGCCA.

Two rounds of consecutive targeting were performed to mutate both alleles using a GFP-Neo- and a GFP-Puro-targeting construct. For electroporation, a single cell suspension of confluent hES cells was prepared using Accutase treatment. Cells were spun at 1,000 r.p.m. and counted.  $8 \times 10^5$  were used for a single electroporation with the 100  $\mu$ l Nucleocuvette Vessels of the 4D-Nucleofector System (Lonza). For electroporation, 100  $\mu$ l of P3-solution (P3 Primary Cell 4D-Nucleofector X Kit) supplemented with Rock inhibitor (10  $\mu$ M; Y-27632, Calbiochem), 2.5  $\mu$ g of CRISPR:hSpCas9 plasmid and 2.5  $\mu$ g of linearized DNA targeting plasmid or 500 ng of each TALEN and 4  $\mu$ g of targeting plasmid were mixed and immediately electroporated using program DC100. Cells from three cuvettes were pooled and plated on one Matrigel coated 10 cm dish in mTeSR1 supplemented with Rock Inhibitor. Selection with neomycin (50  $\mu$ g/ml) or puromycin (0.2  $\mu$ g/ml, both from InvivoGen) was started 2–4 d after plating of the cells. Picking of clones was started 10–14 d after electroporation, and clones were transferred to Matrigel-coated 96-well plates in mTeSR1 plus Rock inhibitor. Rock inhibitor was dismissed 1–2 d after picking. For Southern blot analysis, DNA was isolated from one 48-well for each clone. Three individual *PIEZO2*<sup>-/-</sup> hES cell clones were differentiated and used for immunocytochemistry, qRT-PCR and electrophysiological recordings.

**Generation of hiPS cells.** iPS cells were generated from primary human fibroblasts derived from skin biopsies of healthy donors using a doxycycline-inducible polycistronic lentiviral vector (STEMCCA-OKSM) and a tet-activator M2rtTA-cherry<sup>24,25</sup> (Ethics Committee of Heidelberg University approval no. 2009-350N-MA for hiPS cell generation).

In brief, primary human fibroblasts were seeded at a density of 5,000 cells per well on gelatin coated 6-well plates (BD Biosciences) in fibroblast cell culture medium (DMEM containing 10% FBS, 1 $\times$  nonessential amino acids, 1% penicillin/streptomycin and 50  $\mu$ M 2-mercaptoethanol). For lentiviral transduction 5  $\mu$ l of M2rtTA-cherry and 5  $\mu$ l STEMCCA-OKSM concentrated viral particles were added. To improve the transduction efficiency 1 mg/ml polybrene (Sigma) was supplemented. The following day cells were rinsed with PBS followed by another round of lentiviral transduction. After 24 h the cells were washed

twice with PBS and a 1:1 mixture of fibroblast cell culture medium with human embryonic stem cell (hESC) medium (DMEM/F12 supplemented with 20% KOSR, 1% L-glutamine, 1% penicillin/streptomycin, 1% MEM-NEAA, all Gibco, 0.05 mM 2-mercaptoethanol, Carl Roth, and 10ng/ml bFGF, Promokine) was added. In order to induce the transgene expression the medium was supplemented with 1 µg/mL doxycycline (Sigma). The transduced cells were cultured in the 1:1 mixture medium for one week, afterwards in hESC medium supplemented with 1 µg/mL doxycycline. After 3–5 weeks appearing colonies of reprogrammed cells were picked manually and transferred onto mitomycin c (AppliChem) treated mouse embryonic feeder cells in hESC medium. After another 2 weeks, when the cells reached a stable state, doxycycline was withdrawn and the colonies were further expanded using standard methods for human pluripotent stem cells.

To ensure pluripotency, iPS cells were subjected to a teratoma-formation assay. For this assay iPS cells clump suspension in 140 µL PBS and in 60 µL undiluted Matrigel (30%) was injected subcutaneously into flanks of NOD-SCID mice. Developing teratomas were fixed in 4% formaldehyde overnight and were paraffin embedded. Hematoxylin and eosin sections were analyzed for contributions toward all three germ layers.

**Statistical analysis.** The individual statistical analyses used for the different experiments are stated in the respective methods sections. In general, no statistical

methods were used to predetermine sample sizes, but our sample sizes are similar to those generally employed in the field. Data distribution was assumed to be normal, but this was not formally tested. *t*-tests, when used, were unpaired, two-sided. No corrections for multiple comparisons were performed during the statistical analysis of our results. Initial electrophysiological data, to test mechanosensitive currents in *PIEZO2*<sup>+/+</sup>, *PIEZO2*<sup>+/-</sup> and *PIEZO2*<sup>-/-</sup> LTMRs, were generated by the investigator blind to genotype. Subsequent verification of the absence of mechanosensitive currents in additional cohorts of neurons derived of the three genotypes were performed unblinded. Randomization of samples was as follows: (i) neuronal populations for transcriptome analysis and qRT-PCR (Figs. 2d and 3a) were picked at random by the investigator; (ii) counting of neuronal cells for quantification of the differentiation efficiency was done by defining fields of view at random; (iii) all neurons subjected to electrophysiology recordings (Figs. 4 and 6) were picked at random.

35. Li, H. *et al.* The Sequence Alignment/Map format and SAMtools. *Bioinformatics* **25**, 2078–2079 (2009).
36. Anders, S., Pyl, P.T. & Huber, W. HTSeq—a Python framework to work with high-throughput sequencing data. *Bioinformatics* doi:10.1093/bioinformatics/btu638 (2014).
37. Anders, S. & Huber, W. Differential expression analysis for sequence count data. *Genome Biol.* **11**, R106 (2010).